

Neutron-proton scattering and singular potentials

Mahmut Elbistan^{1*}, Pengming Zhang^{1†} and János Balog^{1,2‡}

¹ *Institute of Modern Physics, Chinese Academy of Sciences,
Lanzhou 730000, China*

² *MTA Lendület Holographic QFT Group, Wigner Research Centre
H-1525 Budapest 114, P.O.B. 49, Hungary*

We consider a Bargmann-type rational parametrization of the nucleon scattering phase shifts. Applying Marchenko's method of quantum inverse scattering we show that the scattering data suggest a singular repulsive core of the potential of the form $2/r^2$ and $6/r^2$ in natural units, for the 3S_1 and 1S_0 channels respectively. The simplest solution in the 3S_1 channel contains three parameters only but reproduces all features of the potential and bound state wave function within one percent error. We also consider the 3S_1 - 3D_1 coupled channel problem with the coupled channel Marchenko inversion method.

*elbistan@impcas.ac.cn

†zhpm@impcas.ac.cn

‡balog.janos@wigner.mta.hu

1 Introduction and motivation

The phenomenological nucleon potential, shown in Fig. 1, is a compilation of many decades' work of nuclear physicists [1, 2, 3]. Although the recent consensus is that the theory of nuclear interactions must be based on effective field theory (for a review, see [4]), the phenomenological potential remains an important source of intuition and often the starting point of quantitative work.

As can be seen in Fig. 1, the phenomenological potential is not unique, since it is constructed to reproduce low energy scattering only. Nevertheless, its main qualitative features are well-established. The force at medium to long range is attractive; this feature has long well been understood in terms of pion and other heavier meson exchange. For a long time the characteristic repulsive core at short distances had no satisfactory theoretical explanation, but with the advance of lattice QCD simulations it became possible to determine the potential in fully dynamical lattice QCD [5, 6]. The lattice results resemble the phenomenological potential, including its repulsive core, obtained for the first time from a first principles calculation. The short distance behaviour of the potential can also be studied in perturbative QCD, thanks to its asymptotic freedom. The results of the perturbative calculations [7, 8] show that at extremely short distances the potential behaves as $1/r^2$ (up to log corrections characteristic to perturbative QCD). Recent calculations in holographic QCD [9] also give an inverse square potential at short distances.

In this paper we study the simple Bargmann-type rational parametrization of the S-matrix and determine the corresponding potential with Marchenko's method of quantum inverse scattering [10, 11]. In this approach (see Appendix B) the potential is given by the formula

$$q(r) = -2 \frac{d^2}{dr^2} \log \mathcal{D}(r), \quad (1.1)$$

where $\mathcal{D}(r)$ is the determinant of a matrix with entries analytic in r . If for small r the determinant is approximately constant,

$$\mathcal{D}(r) = \mathcal{D}_o + \mathcal{O}(r), \quad (1.2)$$

then the corresponding potential is regular at the origin. However, if at $r = 0$ the matrix becomes singular,

$$\mathcal{D}(r) = \mathcal{O}(r), \quad (1.3)$$

then

$$q(r) \sim \frac{\nu(\nu + 1)}{r^2} \quad (1.4)$$

with $\nu = 1$. Thus in this approach the $2/r^2$ type singularity naturally appears. If $\mathcal{D}(r)$ vanishes with a higher power of r , the strength of the singularity ν is larger. Therefore this algebraic method is suitable to study the singular core of the potential.

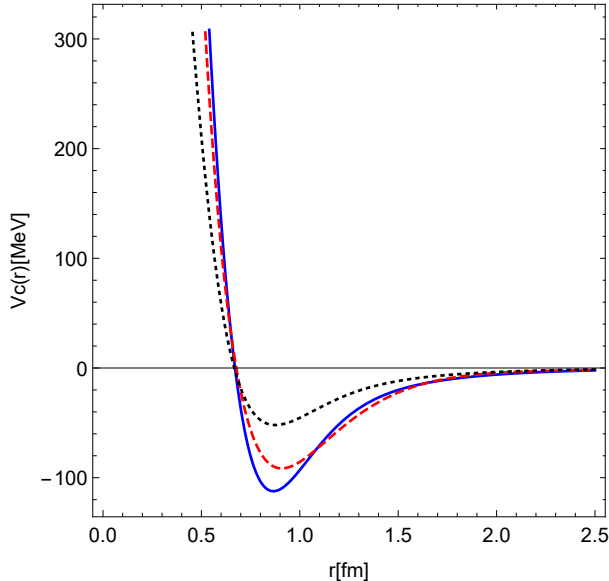


Figure 1: The phenomenological nucleon potential in the 1S_0 channel. The solid (blue) line is the AV18 fit [2], the dashed (red) line is the Reid93 fit [1] and the dotted line (black) is the CDBonn potential [3].

The structure of the paper is as follows. In sect. 2 we study the Bargmann-type representation of the nucleon S-matrix and show that the phase shifts suggest a singular potential. In sect. 3 we work out the simplest description in this class in detail. This representation reproduces the phase shifts with a maximal error of 1.5° and also the deuteron parameters turn out to be correct within 1 percent error. In sect. 4 we present our results for the 3S_1 - 3D_1 coupled channel problem. In sect. 5 we study the 1S_0 channel and discuss the role of the singularity degree. Our conclusions are summarized in sect. 6 while the technical details of our computations are given in the appendices.

2 Bargmann-type parametrization of the nucleon potential

Bargmann-type parametrization [12] of the nucleon potential was already used [13, 14] a long time ago to study nuclear scattering and bound state problems. It has continued to be used ever since to study scattering in various channels, and even for coupled channel problems [15, 16, 17, 18, 19, 20, 21]. In recent studies the methods of SUSY QM (supersymmetric quantum mechanics) has been used, which is also suitable for studying higher angular momentum and coupled channel problems. For a review of SUSY methods in nuclear problems, see [22].

The nucleon scattering phase shifts vanish at zero energy. Originally, also the

vanishing of the phase shifts $\delta(k)$ (modulo π) for scattering at large momentum k and a corresponding regular potential was assumed. Later it was realized that this class naturally contains also $1/r^2$ type singular (repulsive) potentials. In this paper we will focus on the singularity type of the potential and apply the original Marchenko inverse scattering method. The advantage of the Marchenko method is that it gives compact analytic expressions for the potential and the wave function.

The idea of applying Bargmann-type parametrization for the scattering matrix $S(k) = e^{2i\delta(k)}$ originates from the study of the effective range function[§]

$$R(k) = ik \frac{S(k) + 1}{S(k) - 1} = k \cot \delta(k). \quad (2.1)$$

$R(k)$ is an even, real-analytic function of k in a neighbourhood of the origin in the k plane. Analytic continuation for larger momentum values may encounter poles or branch points. Note that in particular, with the exception of the origin, $R(k)$ has a pole where the phase shift vanishes (mod π).

For small momentum, the first two terms

$$R(k) = -\frac{1}{a} + \frac{rk^2}{2} + vk^4 + O(k^6) \quad (2.2)$$

in the low energy expansion give a satisfactory description of the scattering in terms of two parameters: the scattering length a and the effective range r . For larger momentum values one can take into account more terms in this expansion, but a more efficient description, reproducing the poles at larger k values, is provided by a Padé type approximation

$$R(k) = \frac{M(k^2)}{N(k^2)}, \quad (2.3)$$

where M and N are both real polynomials, of degree d_M and d_N , respectively.

This rational function approximation of $R(k)$ is equivalent to a rational parametrization of the scattering matrix of the form

$$S(k) = \prod_{j=1}^N \sigma_{z_j}(k), \quad \sigma_z(k) = \frac{z - ik}{z + ik}, \quad (2.4)$$

where the parameters z_j are the roots of the algebraic equation

$$M(-z^2) + zN(-z^2) = 0. \quad (2.5)$$

We see that the property $S(0) = 1$ is built in, but the phase shift at large energies depends on the parity of the number of roots,

$$S(\infty) = (-1)^N. \quad (2.6)$$

[§]This formula for the effective range function is valid for the s-wave only. For the d-wave we have to use the modified form (4.3).

If for large momentum

$$S(k) = 1 + O(1/k), \quad (2.7)$$

then the effective range function diverges for large k like $O(k^2)$. If however for large momentum

$$S(k) = -1 + O(1/k), \quad (2.8)$$

then $R(k)$ approaches a constant at large k . Thus $[d_M/d_N]$, the type of the Padé approximation, is related to the large energy behaviour of the phase shift and, due to Levinson's theorem, to the short distance singularity of the potential. (See Appendix A.)

In Ref. [15] the effective range function for neutron-proton scattering in the triplet (3S_1) channel was parametrized as

$$R_t(k) = -\frac{1}{a_t} + \frac{r_t k^2}{2} + \frac{v_t k^4}{1 - k^2/k_o^2} \quad (2.9)$$

with

$$a_t = 5.4030 \text{ fm}, \quad r_t = 1.7494 \text{ fm}, \quad v_t = 0.163 \text{ fm}^3. \quad (2.10)$$

The scattering length a_t and the effective range r_t were obtained from the measured low energy phase shifts and the position of the pole at $k = k_o = 2.1057 \text{ fm}^{-1}$ was determined from the vanishing of the phase shift (see Fig. 2). Finally, the shape parameter v_t was fitted to the measured phase shifts in the range of laboratory neutron energies up to 350 MeV.

This parametrization is a [2/1] type Padé fit, which can also be written in the form

$$R_t(k) = \frac{w_0 + w_1 k^2 + w_2 k^4}{1 - k^2/k_o^2}, \quad (2.11)$$

where (using fm units)

$$w_0 = -0.1851, \quad w_1 = 0.9164, \quad w_2 = -0.0343. \quad (2.12)$$

The corresponding S-matrix has four roots z_j ($\mathcal{N} = 4$). For large k , $R_t(k) = O(k^2)$ and $S(\infty) = 1$. However, the coefficient w_2 is extremely small. We take it as an indication that we get a better description if

$$R_t(k) \rightarrow \text{const.}, \quad S(\infty) = -1. \quad (2.13)$$

In ref. [18] a [2/2] type Padé fit with $\mathcal{N} = 5$ corresponding to $S(\infty) = -1$ was studied. In the next section we use a [1/1] type Padé approximation, which is the simplest possibility with property (2.13).

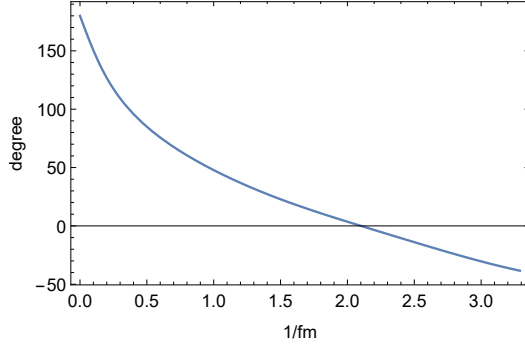


Figure 2: Neutron-proton scattering phase shifts in the 3S_1 channel as function of the centre of mass momentum [23].

3 Simplest Bargmann representations

3.1 A simple [1/1] type Padé fit

Motivated by the above observations we make a simple [1/1] type Padé fit to the scattering data.

We use the nucleon scattering phase shifts from the publicly available GWDAC data base [23] (SM16 solution). The 3S_1 channel neutron-proton phase shifts are shown in Fig. 2. The phase shifts $\delta(k)$ are shown (in degrees) as function of the centre of mass wave number k corresponding to neutron laboratory kinetic energies in the range $0 \leq T \leq 900$ MeV. We will measure distances (wave numbers) in fm (fm^{-1}) units, energies and potentials in MeV.

The phase shifts are decreasing with energy, starting from $\delta(0) = 180^\circ$, which corresponds to $S(0) = 1$. The phase shift vanishes at $T = 366.28$ MeV, corresponding to $k = k_o = 2.1007 \text{ fm}^{-1}$. Here the phase shifts change sign and continue to decrease with energy.

Fitting to the low energy data in the range $0 \leq T \leq 10$ MeV we find the scattering length/effective range parameters[¶]

$$a_t = 5.4028 \text{ fm}, \quad r_t = 1.7495 \text{ fm}. \quad (3.1)$$

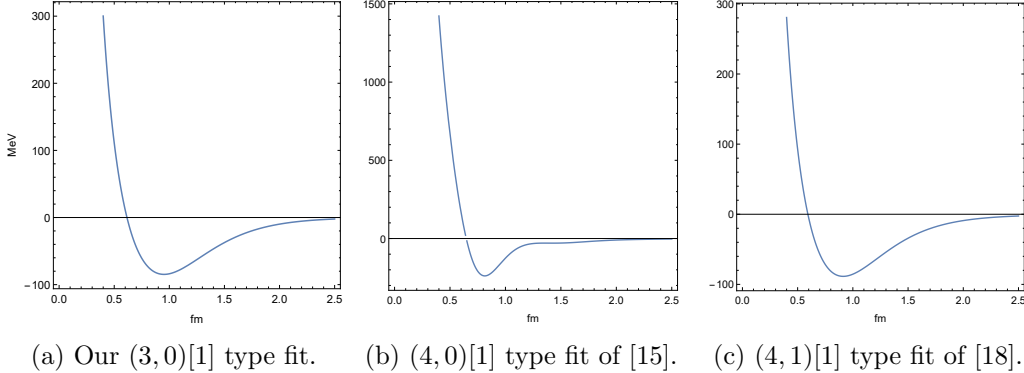
To make the [1/1] type Padé fit, we need no additional parameters beyond the well-established set (3.1) and k_o . We find

$$R_t(k^2) = -\frac{1}{a_t} \frac{1 - (a_t r_t/2 + 1/k_o^2)k^2}{1 - k^2/k_o^2} = -\frac{1}{a_t} \frac{1 - 4.9527 k^2}{1 - 0.2266 k^2}. \quad (3.2)$$

This gives for the next coefficient in the low energy expansion (2.2) the value

$$v_t = \frac{r_t}{2k_o^2} = 0.1982 \text{ fm}^3, \quad (3.3)$$

[¶]Our results differ slightly from those of Ref. [15] because we use recent experimental data.



(a) Our (3,0)[1] type fit. (b) (4,0)[1] type fit of [15]. (c) (4,1)[1] type fit of [18].

Figure 3: Nucleon potentials from different Padé fits. Note that the scale used in panel (b) is different from the other two due to the very different shape and range of the potential.

not very different from (2.10). Using (3.2) gives a reasonable fit to the phase shifts $\delta(k)$ up to laboratory energies 350 MeV, with errors not exceeding 1.4° .

The S-matrix corresponding to (3.2) contains three factors

$$S(k) = \sigma_a(k)\sigma_b(k)\sigma_c(k) \quad (3.4)$$

with $a = 1.5813$, $b = 0.23135$, $c = 2.2327$. We can interpret the S-matrix pole at $k = ib$ as corresponding to the deuteron bound state since this b value is very close to $b_o = 0.2316$, obtained from the deuteron binding energy

$$E_d = \frac{\hbar^2 b_o^2}{2m} = 2.2245 \text{ MeV.} \quad (3.5)$$

Here $m = 469.459 \text{ MeV}/c^2$ is the reduced mass of the np system.

To characterize a system described by the rational S-matrix (2.4) we will use the notation $(\mathcal{N}_+, \mathcal{N}_-)[J]$, where \mathcal{N}_\pm is the number of factors σ_{z_j} with z_j having positive (negative) real parts and J is the number of bound states. Thus our simple fit is of type (3,0)[1]. Further, we can argue that the would-be leading exponential e^{-2br} must be absent from the potential, since this would give a much slower decay at infinity than expected (the Yukawa tail of the potential dominated by pion exchange). This will happen if this S-matrix pole is an inner one (see Appendix A), in which case no new bound state parameters need to be introduced.

The solution of the inverse scattering problem corresponding to (3.4) is discussed in Appendix B.4. The solution is based on a 2×2 matrix inversion and can be given analytically.

Let us define

$$Y_a(r) = \frac{(b-a)(c-a)}{(b+a)(c+a)} e^{2ar} - 1, \quad Y_c(r) = \frac{(a-c)(b-c)}{(a+c)(b+c)} e^{2cr} - 1 \quad (3.6)$$

and

$$\tilde{\mathcal{D}}(r) = Y_a(r)Y_c(r) - \frac{4ac}{(a+c)^2}. \quad (3.7)$$

Then the potential (in fm units) is

$$q(r) = -2 \frac{d^2}{dr^2} \ln |\tilde{\mathcal{D}}(r)|. \quad (3.8)$$

It is shown in Fig. 3a. It closely resembles the phenomenological potential. It has a single minimum -84.7 MeV at $r = 0.952$ fm and is singular for $r \rightarrow 0$ behaving as

$$V(r) \sim \frac{\hbar^2}{2m} \left(\frac{2}{r^2} - 4.95 + O(r) \right) = 41.47 \left(\frac{2}{r^2} - 4.95 + O(r) \right) \text{ MeV}. \quad (3.9)$$

We also calculated the ground state wave function.

$$\psi_o(r) = \sqrt{\tilde{R}_b} f_o(r), \quad f_o(r) = e^{-br} \left\{ 1 + \frac{4acB}{\tilde{\mathcal{D}}} \right\}, \quad (3.10)$$

where

$$\tilde{R}_b = 2b \frac{(a+b)(c+b)}{(a-b)(c-b)} \quad (3.11)$$

and

$$B = \frac{1}{a+b} \left\{ \frac{Y_c}{2c} + \frac{1}{a+c} \right\} + \frac{1}{c+b} \left\{ \frac{Y_a}{2a} + \frac{1}{a+c} \right\}. \quad (3.12)$$

In addition to the asymptotic constant A_o characterising the large distance decay of the wave function,

$$\psi_o(r) \sim A_o e^{-br}, \quad (3.13)$$

we have also calculated the root-mean-square “matter” radius of the deuteron, defined by

$$(2r_m)^2 = \int_0^\infty r^2 \psi_o^2(r) dr. \quad (3.14)$$

We find

$$A_o = 0.8746 \text{ fm}^{-1/2}, \quad r_m = 1.9441 \text{ fm}. \quad (3.15)$$

Again, we find very good agreement^{||} with experimental data [24],

$$A_o^{\text{exp}} = 0.8845(8) \text{ fm}^{-1/2}, \quad r_m^{\text{exp}} = 1.9676(10) \text{ fm}. \quad (3.16)$$

^{||}Actually, the agreement is even better with an older determination of these constants: $A_o = 0.8781(44)$, $r_m = 1.9580(61)$ [25].

3.2 Higher Padé approximations

For comparison, we have also constructed the potential and wave function corresponding to the fits in Refs. [15] and [18].

The fit in Ref. [15] is of the form

$$R_t(k^2) = -\frac{1}{a_t} \frac{(1 - 4.9138 k^2)(1 - 0.0377 k^2)}{1 - 0.2255 k^2}, \quad (3.17)$$

reproducing the low energy expansion parameters (2.10).

This [2/1] type Padé fit leads to the S-matrix

$$S(k) = \sigma_a(k)\sigma_b(k)\sigma_c(k)\sigma_d(k) \quad (3.18)$$

with $a = 1.2293$, $b = 0.2315$, $c = 2.5603 + 3.5248i$, $d = c^*$. Identifying b again with the deuteron pole and assuming the absence of this exponent from the potential leads to an inverse scattering problem of type (4,0)[1]. (See Appendix B.5.)

Although (3.17) gives better overall fit to the scattering data (the errors in the phase shifts in the laboratory energy range $0 \leq T \leq 350$ MeV are less than 0.5°), the resulting potential, shown in Fig. 3b, is very different from the phenomenological one. It is much steeper, has a deep minimum -238.8 MeV at $r = 0.814$ and is more singular at the origin:

$$V(r) \sim 41.47 \left(\frac{6}{r^2} + 4.11 + O(r) \right) \text{ MeV.} \quad (3.19)$$

We have also constructed the deuteron wave function and calculated the parameters

$$A_o = 0.8763 \text{ fm}^{-1/2}, \quad r_m = 1.9442 \text{ fm.} \quad (3.20)$$

The (4,1)[1] type S-matrix (see Appendix B.5) of Ref. [18] has parameters

$$a = -0.45146, \quad b = 0.23154, \quad c = 0.43654, \quad d = 1.6818, \quad e = 2.3106 \quad (3.21)$$

giving the [2/2] type

$$R_t(k^2) = -\frac{1}{a_t} \frac{(1 - 4.8846 k^2)(1 + 4.8594 k^2)}{(1 - 0.2104 k^2)(1 + 4.9431 k^2)} \quad (3.22)$$

and low energy expansion parameters

$$a_t = 5.4220 \text{ fm}, \quad r_t = 1.7550 \text{ fm}, \quad v_t = 0.0329 \text{ fm}^3. \quad (3.23)$$

The potential is shown in Fig. 3c and it is again very similar to the phenomenological one with minimum -88.6 MeV at $r = 0.913$ and short distance asymptotics

$$V(r) \sim 41.47 \left(\frac{2}{r^2} - 5.40 + O(r) \right) \text{ MeV.} \quad (3.24)$$

The deuteron parameters are

$$A_o = 0.8854 \text{ fm}^{-1/2}, \quad r_m = 1.9568 \text{ fm.} \quad (3.25)$$

4 Coupled channel nucleon-nucleon potential

In section 3.1 we presented a Bargmann type S-matrix which has only three poles (3.4). As can be seen from Fig. 3a, this representation describes the 3S_1 channel of the neutron-proton scattering quite well.

However, the complete problem of triplet neutron-proton scattering includes both the 3S_1 and 3D_1 channels which are coupled to each other. In order to solve it completely, we also need the data for the d-wave phase shifts and the mixing angle of the channels. In addition, we have to employ the multichannel Marchenko method [19, 20] for this inverse scattering (see appendix C).

Our 2-channel inversion procedure is based on the 2×2 scattering matrix $S(k)$ which can be decomposed as

$$S(k) = O(k) \operatorname{diag}(e^{2i\delta_1(k)}, e^{2i\delta_2(k)}) O^T(k), \quad (4.1)$$

where $O(k)$ is an $SO(2)$ matrix,

$$O(k) = \begin{pmatrix} \cos \epsilon(k) & -\sin \epsilon(k) \\ \sin \epsilon(k) & \cos \epsilon(k) \end{pmatrix}. \quad (4.2)$$

$e^{2i\delta_1(k)}$ and $e^{2i\delta_2(k)}$ are the scattering matrices for the 3S_1 and 3D_1 channels, respectively.

For the 3S_1 channel scattering matrix we will use the results of section 3. First we take for $A(k) = e^{2i\delta_1(k)}$ (3.4) and later alternatively (3.18) and the one parametrized by the roots (3.21).

In order to determine $B(k)$ we downloaded the experimental 3D_1 phase shift data from [23]. The simplest parametrization of the d-wave scattering matrix $B(k) = e^{2i\delta_2(k)}$ needs 5 poles because it is an $\ell = 2$ partial wave and in the limit $k \rightarrow 0$ it has to satisfy $B(k) = 1 + O(k^5)$. Writing the effective range function as

$$R_d(k) = k^5 \cot \delta_2(k) = ik^5 \frac{B(k) + 1}{B(k) - 1} = c_o + c_1 k^2 + c_2 k^4 \quad (4.3)$$

we conclude that there are only 3 independent parameters in the simplest solution for $R_d(k)$. Fitting the three parameters in (4.3), we obtain the following scattering phase:

$$B(k) = \sigma_a(k) \sigma_b(k) \sigma_c(k) \sigma_d(k) \sigma_e(k), \quad (4.4)$$

with poles at $a = -0.43936 - 0.47933i$, $b = a^*$, $c = 0.42490 - 0.52554i$, $d = c^*$, $e = 4.5931$. Like its s-wave counterpart, the d-wave scattering matrix (4.4) has the asymptotic value $B(\infty) = -1$. However, it has no bound states.

In Fig. 4a, we compare our d-wave phase shift fit with the one in [18]. Although our poles are quite different, our fit is compatible with the one in [18].

For the mixing angle $\epsilon(k)$, once again, we use the recent experimental data from [23]. We fit them to the functional form

$$\epsilon(k) = \arctan \left[\frac{f_1 k^2}{e_1^2 + f_1^2 - e_1 k^2} \right] + \arctan \left[\frac{f_2 k^2}{e_2^2 + f_2^2 - e_2 k^2} \right], \quad (4.5)$$

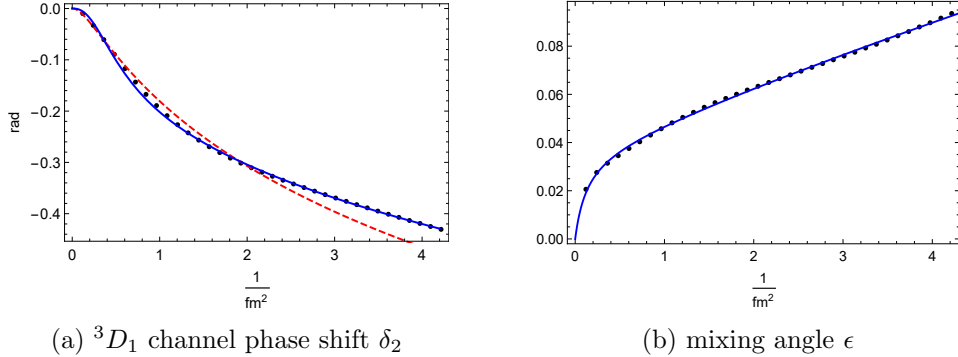


Figure 4: δ_2 and ϵ as functions of the centre of mass momentum squared [23]. In both figures, the solid (blue) line represents our fit and the dots represent the data. On the left, the dashed (red) line is the fit used in [18].

with the constraint

$$\eta = \tan \beta = 0.0254, \quad \beta = -\epsilon(ib). \quad (4.6)$$

Here we took, for simplicity, the value $b = 0.23135$ from our simplest fit** and found

$$E_1 = e_1 + if_1 = -0.13304 + 0.004879i \quad \text{and} \quad E_2 = e_2 + if_2 = -34.88 + 36.13i, \quad (4.7)$$

where $E_{1,2}$ are two complex energies parametrizing

$$z(k) = \prod_{m=1}^2 \frac{1 - k^2/E_m^*}{1 - k^2/E_m}. \quad (4.8)$$

This form solves the constraints (C.49) and (C.25) for $z(k) = e^{-2i\epsilon(k)}$. Fig. 4b shows our fit for the mixing angle. We found that already 2 (complex) parameters in (4.8) give a satisfactory fit. Using 3 parameters there is only marginal improvement.

We have 3 poles from the 3S_1 channel (3.4) with one of them being the bound state. From the 3D_1 channel (4.4), we get 5 poles, however only 3 of them are located in the upper half of the complex plane. From $z(k)$ and its inverse we get 4 poles in the upper half plane. As a result, the Marchenko equation is transformed to a linear problem with 9 residues which we solved algebraically. We present our final results in Fig. 5. In this and the following figures, V_{11} represents the $\ell = 0$, V_{22} the $\ell = 2$, and V_{12} the mixed component of the 2×2 potential matrix.

We also studied the same problem using (3.18) of Ref. [15] for the s-wave part while keeping our d-wave parameters (4.4) and the mixing angle (4.5). In this parametrization, we have 10 residues. The results are shown in Fig. 6.

Lastly, we take the s-wave roots (3.21) of Ref. [18] and use our d-wave parameters (4.4) and the mixing angle (4.5). This is, again, a coupled problem with 10 poles. We plot these results in Fig. 7.

**The experimental value for the deuteron mixing parameter $\eta = 0.0254(2)$ was taken from [26].

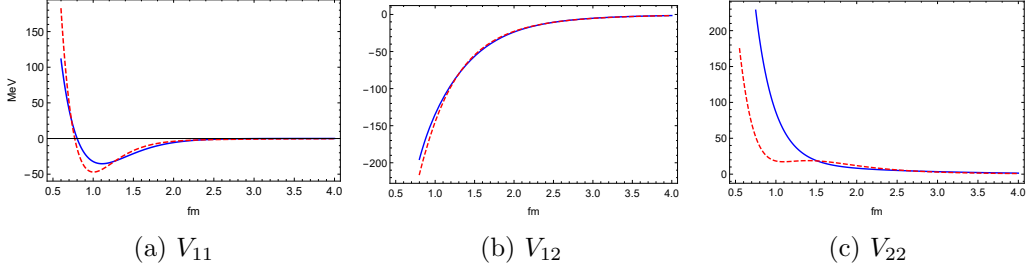


Figure 5: Matrix elements of the 3S_1 - 3D_1 scattering potential. The solid (blue) line represents our results and the dashed (red) line belongs to the Reid93 potential.

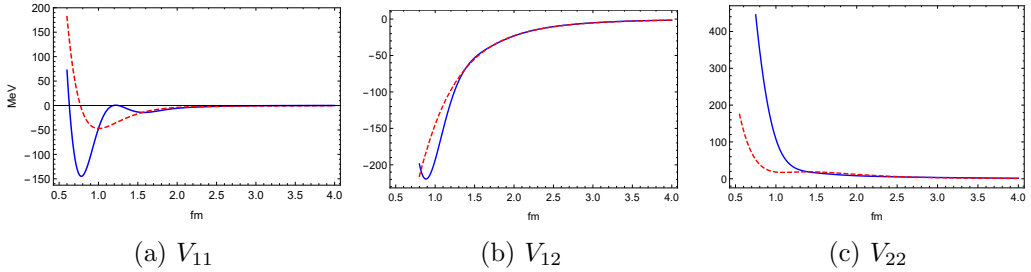


Figure 6: 3S_1 - 3D_1 scattering potential obtained from the s-wave data in [15]. The solid (blue) line is the result of our multi-channel calculations.

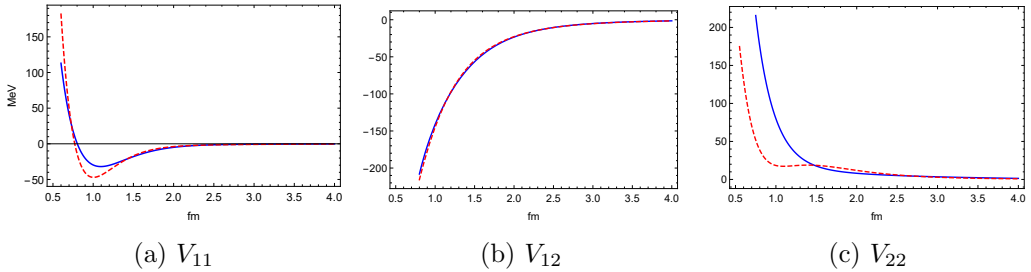


Figure 7: 3S_1 - 3D_1 scattering potential generated from the s-wave data in [18].

Focusing on the s-wave components of potential matrices, we see that Fig. 5a and Fig. 7a are very similar and closely resemble the phenomenological potential while the solution shown in Fig. 6a is different, very deep and steeply rising for small r . Our conclusion after including the mixing effects is thus unchanged: the data strongly suggest a singular potential with strength parameter $\nu = 1$ in the 3S_1 np channel.

5 1S_0 partial wave and potential

In this section we consider the 1S_0 partial wave of the neutron-proton scattering as a relevant physical example without multi-channel mixing. We again concentrate on the role of the strength of the short distance singularity ν .

We begin our discussion with reviewing former studies, which were based on SUSY quantum mechanics.

In [21] the S-matrix

$$S_1(k) = \sigma_a(k)\sigma_b(k)\sigma_c(k)\sigma_d(k)\sigma_e(k), \quad (5.1)$$

with the roots $a = -0.040$, $b = -0.837$, $c = 0.581$, $d = 1.453 + 1.313i$, $e = d^*$ is proposed. According to Levinson's theorem (A.43), the singularity degree is $\nu = 1$. Therefore, the resulting potential has the form $U \rightarrow \frac{2}{r^2}$ in the limit $r \rightarrow 0$. Our calculations with the Marchenko method are presented in Fig. 8a.

However, the correct short range behavior of the potential, as suggested by [27], should be $U \rightarrow \frac{6}{r^2}$ corresponding to a singularity degree $\nu = 2$. Indeed, in [27] such a scattering matrix with 6 poles is considered:

$$S_2(k) = \sigma_a(k)\sigma_b(k)\sigma_c(k)\sigma_d(k)\sigma_e(k)\sigma_f(k), \quad (5.2)$$

$a = -0.0401$, $b = -0.7540$, $c = 0.6152$, $d = 2.0424$, $e = 4.1650$, $f = 4.6000$. We derived the associated potential and plot it in Fig. 8b. As it can be seen directly from the figure, when the singularity degree is correct, the resulting potential has a good match with the phenomenological potential.

We have made some new fits to the same problem. We consider first the simplest fit with a minimal number of parameters, which we calculated analogously to the method leading to (3.4) and found the following S-matrix:

$$S_3(k) = \sigma_a(k)\sigma_b(k)\sigma_c(k), \quad (5.3)$$

with one of the poles in the lower half plane: $a = -0.04007$, $b = 1.1061$, $c = 2.9254$. According to Levinson's theorem, the related singularity degree is $\nu = 1$. Here we can use simple formulas similar to the ones in subsect. 3.1 to derive the potential, which is plotted in Fig. 9a. As clearly seen from the figure, the potential has a wrong short range behavior although in the long range there is a good match.

Since the simplest 3-parameter fit is not satisfactory here, we next considered a fit with four parameters. We found

$$S_4(k) = \sigma_a(k)\sigma_b(k)\sigma_c(k)\sigma_d(k), \quad (5.4)$$

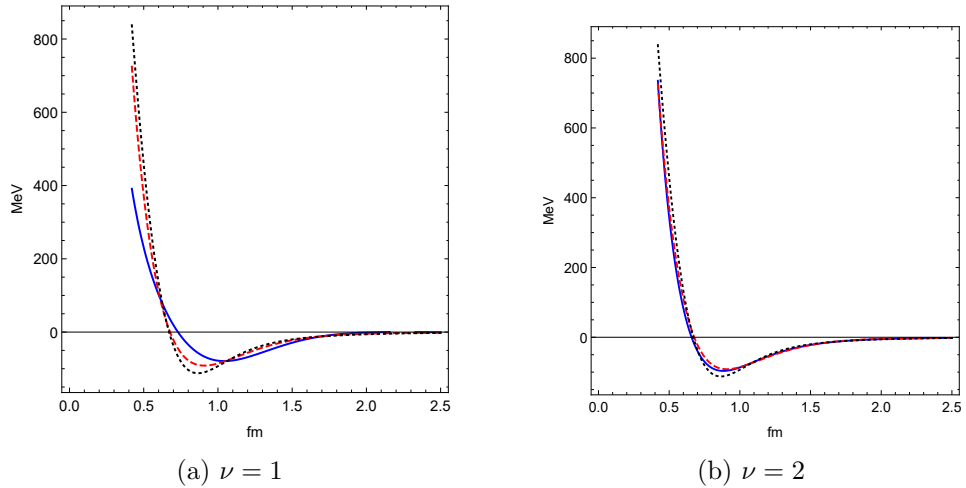


Figure 8: 1S_0 potential. The solid (blue) lines represent the results in the cited papers, the dashed (red) line is the Reid93 and the dotted (black) line is the AV18 reference potential.

with $a = -0.04034$, $b = 1.4561$, $c = 5.2856$, $d = 4.9680$. This scattering matrix yields a potential with the correct singularity degree $\nu = 2$. We plot our result in Fig. 9b.

We see that, similarly to the 3S_1 - 3D_1 problem studied in sections 3 and 4, increasing the number of fit parameters makes the shape of the potential better only if the correct singularity strength is ensured. In the 1S_0 example discussed in this section the 3 and 5 parameter solutions both have $\nu = 1$ and disagree with the phenomenological potential for small r whereas the 4 and 6 parameter solutions (both with $\nu = 2$) give nearly equally good description of the potential, including the repulsive core.

6 Conclusion

In this paper we have shown that scattering data for the triplet channel nucleon scattering strongly suggest a singular potential with inverse square type singularity and strength $2/r^2$. In this class of potentials already the simplest 3-parameter Bargmann-type fit reproduces all qualitative features of the phenomenological potential. In this case the potential and the deuteron wave function can be given in very simple analytic form. Deuteron data are also reproduced within 1 percent error and this representation of the phase shifts gives a maximal error of 1.5° in the energy range between 0 and 350 MeV.

We have compared our results to the 4 and 5-parameter fits of Refs. [15] and [18] respectively. With more parameters the agreement with the phase shifts and deuteron parameters is of course better, but while the effective range functions ((3.17) and (3.22) respectively) both look like small refinements of (3.2) of the

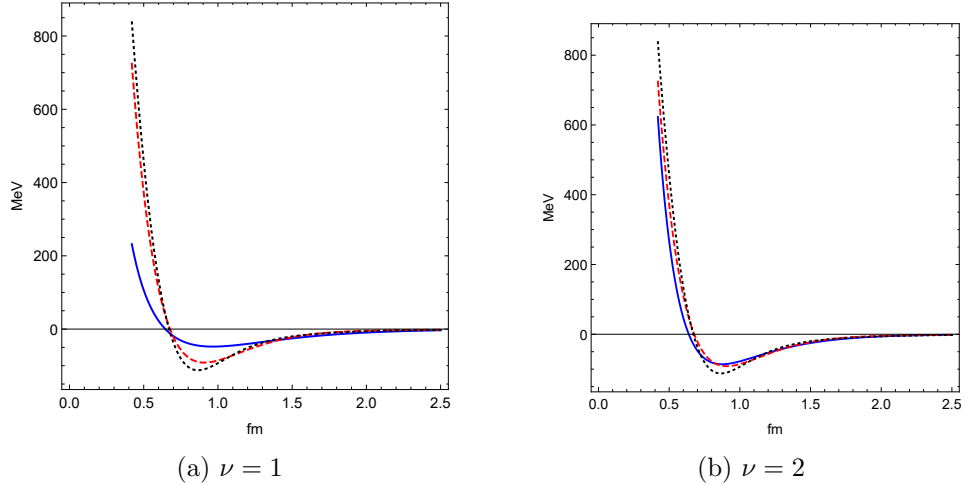


Figure 9: 1S_0 potential. The solid (blue) lines represent our results, the dashed (red) line is the Reid93 and the dotted (black) line is the AV18 reference potential.

simplest fit only, there is a drastic difference between the two cases. While the 5-parameter solution shows no qualitative difference from our simple case, the 4-parameter solution is very different, the potential has a very different shape, it is more singular and steeper. The reason is that while the simplest 3-parameter potential and the 5-parameter one both go like $2/r^2$ for short distances, the 4-parameter one has a much stronger $6/r^2$ singularity.

Although the triplet scattering is really a coupled channel problem, we have demonstrated that the above conclusion remains unchanged after the coupling to the higher angular momentum d-wave and taking account of the mixing of the two channels.

We have also studied the same questions in the singlet channel and found that the correct singularity strength is also important there. However, the correct singularity turns out to be $6/r^2$. This is expected since the interaction must be more repulsive in this channel.

We have applied the Marchenko method of inverse scattering to construct the potential and wave function from Bargmann-type rational representation of the scattering matrix. We have shown that this method is very effective, because the Marchenko integral equation in this case is reduced to an algebraic problem of matrix inversion and gives compact analytical expressions for both the potential and the wave function. Our determinant formula (B.23) closely resembles the analogous Crum-Krein formula used in SUSY quantum mechanics [22] but the interesting question of finding an explicit mapping between them will be left for future studies.

Acknowledgments

We thank A. M. Shirokov for discussions. This work was supported by the National Natural Science Foundation of China (Grant No. 11575254), by the Chinese Academy of Sciences President's International Fellowship Initiative (Grant No. 2017PM0045 and Grant No. 2017VMA0041) and by the Hungarian National Science Fund OTKA (under K116505). J. B. would like to thank the CAS Institute of Modern Physics, Lanzhou, where most of this work has been carried out, for hospitality.

A Scattering and inverse scattering for singular potentials

In this appendix we consider the scattering theory in the ℓ th partial wave, where the angular momentum quantum number ℓ is a nonnegative integer. The theory of quantum inverse scattering [28, 29, 10] in the case of regular potentials is well established. Here we closely follow the method of Ref. [11], with modifications necessary for potentials singular at the origin. Although in this paper all applications are based on rational S-matrices and the corresponding singularity strength values are integers, for completeness we discuss the general case of arbitrary $\nu \geq 0$.

We begin with the radial Schrödinger equation

$$-\frac{\hbar^2}{2m}u''(r) + \frac{\hbar^2}{2m} \frac{\ell(\ell+1)}{r^2}u(r) + V(r)u(r) = Eu(r), \quad (\text{A.1})$$

where m is the reduced mass, V is the interaction potential and E is the total energy of the particles. We introduce

$$q(r) = \frac{2m}{\hbar^2}V(r), \quad k^2 = \frac{2mE}{\hbar^2}, \quad U(r) = q(r) + \frac{\ell(\ell+1)}{r^2}, \quad (\text{A.2})$$

which allows us to simplify (A.1) as

$$-u''(r) + U(r)u(r) = k^2u(r). \quad (\text{A.3})$$

We will consider potentials which are singular at the origin and vanish exponentially at large distances,

$$q(r) \sim \frac{\beta_o}{r^2} + \mathcal{O}(1), \quad r \rightarrow 0, \quad (\text{A.4})$$

$$q(r) \sim e^{-2\kappa r}, \quad r \rightarrow \infty, \quad (\kappa > 0). \quad (\text{A.5})$$

The small r singularity of the total potential term in (A.3) is determined by the parameter ν defined by

$$\nu(\nu+1) = \beta_o + \ell(\ell+1), \quad (\text{A.6})$$

such that

$$U(r) \sim \frac{\nu(\nu+1)}{r^2} + O(1), \quad r \rightarrow 0, \quad (\text{A.7})$$

$$U(r) \sim \frac{\ell(\ell+1)}{r^2} + \text{exp. small}, \quad r \rightarrow \infty. \quad (\text{A.8})$$

A.1 Solutions of the direct scattering problem

We will use two special solutions of the Schrödinger equation (A.3), which are specified according to their behaviour near the origin or at infinity.

The regular solution* $\varphi(r, k) \equiv \varphi_k(r)$ is vanishing at $r = 0$ like

$$\varphi_k(r) \sim Dr^{\nu+1} \quad r \rightarrow 0, \quad (\text{A.9})$$

where the constant D is chosen for later convenience as

$$D = \frac{\sqrt{\pi}}{2^{\nu+1}\Gamma(\nu+3/2)}. \quad (\text{A.10})$$

The regular solution is a real analytic and even function of k for all complex k :

$$\varphi_k^*(r) = \varphi_{k^*}(r) \quad \text{and} \quad \varphi_k(r) = \varphi_{-k}(r). \quad (\text{A.11})$$

The Jost solution $f(r, k) \equiv f_k(r)$ is determined by its asymptotic behaviour

$$f_k(r) \sim e^{ikr}, \quad r \rightarrow \infty. \quad (\text{A.12})$$

It is well-defined in the upper half plane, $\text{Im } k \geq 0$ ($k \neq 0$) and it is analytic for $\text{Im } k > 0$. $f_k(r)$ satisfies the property

$$f_k^*(r) = f_{-k^*}(r). \quad (\text{A.13})$$

The Jost function $f(k)$ is the Wronskian determinant of the regular solution and the Jost solution

$$f(k) = W[\varphi_k, f_k] = \varphi'_k f_k - \varphi_k f'_k, \quad (\text{A.14})$$

where for any two solutions of the Schrödinger equation (with the same k) the Wronskian is defined by

$$W[\psi_1, \psi_2] = \psi'_1 \psi_2 - \psi_1 \psi'_2 \quad (\text{A.15})$$

and is a constant. The Jost function is well-defined in the upper half plane i.e. $\text{Im } k \geq 0$ ($k \neq 0$) and analytic for $\text{Im } k > 0$. It also satisfies

$$f^*(k) = f(-k^*) \quad (\text{A.16})$$

*Note that the generic solution is singular at $r = 0$ like $r^{-\nu}$.

and it cannot vanish for real nonzero k .

For real k the regular solution $\varphi_k(r)$ can be written as a linear combination of $f_k(r)$ and $f_{-k}(r)$ as

$$\varphi(r, k) = \frac{i}{2k} [f(k)f_{-k}(r) - f(-k)f_k(r)], \quad (k \neq 0). \quad (\text{A.17})$$

For real k it is useful to introduce the phase and modulus of the Jost function by

$$f(k) = |f(k)| e^{-i\tilde{\delta}(k)}. \quad (\text{A.18})$$

The large r asymptotics of the real solution can then be written as

$$\varphi_k(r) \sim \frac{|f(k)|}{k} \sin[kr + \tilde{\delta}(k)]. \quad (\text{A.19})$$

A.2 The $\frac{\nu(\nu+1)}{r^2}$ potential

The solution of (A.3) with $U(r) = \frac{\nu(\nu+1)}{r^2}$ can be given in terms of Bessel and Hankel functions. (Note that for $\nu = \ell$ this is the free case, i.e. $q(r) = 0$, but for generic ν the potential is not in our class (A.7-A.8).) The Hankel functions are

$$H_\alpha^{(1,2)}(x) = J_\alpha(x) \pm iY_\alpha(x) \quad (\text{A.20})$$

where J_α and Y_α are the Bessel functions and we define the rescaled Hankel functions

$$h_\nu(x) = \sqrt{\frac{\pi x}{2}} H_\alpha^{(1)}(x), \quad \tilde{h}_\nu(x) = \sqrt{\frac{\pi x}{2}} H_\alpha^{(2)}(x), \quad (\text{A.21})$$

where $\alpha = \nu + 1/2$. Their asymptotic behaviour for large arguments is

$$h_\nu(x) \sim e^{-\frac{i(\nu+1)\pi}{2}} e^{ix}, \quad \tilde{h}_\nu(x) \sim e^{\frac{i(\nu+1)\pi}{2}} e^{-ix} \quad (\text{A.22})$$

in the upper and lower half planes, respectively. For integer ℓ , h_ℓ and \tilde{h}_ℓ are given by the finite series

$$h_\ell(x) = (-i)^{\ell+1} e^{ix} \sum_{m=0}^{\ell} \frac{i^m}{m!(2x)^m} \frac{(\ell+m)!}{(\ell-m)!}, \quad (\text{A.23})$$

$$\tilde{h}_\ell(x) = i^{\ell+1} e^{-ix} \sum_{m=0}^{\ell} \frac{(-i)^m}{m!(2x)^m} \frac{(\ell+m)!}{(\ell-m)!}. \quad (\text{A.24})$$

The regular and Jost solutions in this case are

$$\varphi_k(r) = k^{-\alpha} \sqrt{\frac{\pi r}{2}} J_\alpha(kr), \quad f_k(r) = e^{\frac{i(\nu+1)\pi}{2}} h_\nu(kr) \quad (\text{A.25})$$

respectively, and so in the upper half plane ($\text{Im } k \geq 0$)

$$f(k) = (-ik)^{-\nu} \quad (\text{A.26})$$

and for real k

$$\tilde{\delta}(k) = -\frac{\nu\pi}{2}\text{sgn}(k). \quad (\text{A.27})$$

This is not continuous at $k = 0$.

For $\nu = \ell$, $k^\ell f_k(r)$ is an entire function and

$$\sigma(k) = \frac{f(-k)}{f(k)} = (-1)^\ell. \quad (\text{A.28})$$

A.3 Analytic extension

It can be shown [11] that the Jost solution also satisfies an integral equation and with the help of this integral equation the rescaled Jost solution

$$\mathcal{F}(r, k) = (-ik)^\ell f(r, k) \quad (\text{A.29})$$

can be analytically extended from the upper half plane to the larger region $\text{Im } k > -\kappa$. Moreover, in a neighbourhood of the origin (small k) $\mathcal{F}(r, k)$ can be written as

$$\mathcal{F}(r, k) = \mathcal{A}(r, k) + ik^{2\ell+1} \mathcal{B}(r, k), \quad (\text{A.30})$$

where $\mathcal{A}(r, k)$ and $\mathcal{B}(r, k)$ are real analytic and even there.

$\mathcal{F}(k)$, $A(k)$ and $B(k)$ have analogous properties, where

$$\mathcal{F}(k) = (-ik)^\ell f(k) = A(k) + ik^{2\ell+1} B(k). \quad (\text{A.31})$$

Finally for real k we write

$$\mathcal{F}(k) = |\mathcal{F}(k)| e^{-i\delta(k)} \quad (\text{A.32})$$

and (for $k > 0$) we see that

$$\tilde{\delta}(k) = \delta(k) - \frac{\pi\ell}{2} \quad (\text{A.33})$$

so $\delta(k)$ measures the deviation from the free case.

$A(k)$ and $B(k)$ can be Taylor expanded for small k as

$$A(k) = A_o + A_1 k^2 + \dots, \quad B(k) = B_o + B_1 k^2 + \dots \quad (\text{A.34})$$

It can be shown that if $A_o = 0$ ($\mathcal{F}(0) = 0$) then the zero energy regular solution is bounded. For $\ell \geq 1$ it is even normalizable, so in this case there is a genuine zero energy bound state. Since in our applications we never encounter zero energy bound states (nor bounded zero energy solutions for $\ell = 0$), we will assume that $A_o \neq 0$ and these are absent. All our subsequent considerations are valid under this assumption.

A.4 Negative energy bound states

Negative energy bound states with energy $-\kappa_j^2$ can be identified with zeros of the Jost function on the positive imaginary axis

$$f(i\kappa_j) = 0, \quad \kappa_j > 0, \quad j = 1, \dots, J. \quad (\text{A.35})$$

In this case the regular solution $\varphi(r, i\kappa_j) \equiv \varphi_j(r)$ is real and proportional to the Jost solution $f_j(r) = f(r, i\kappa_j)$ and thus normalizable. The normalization constant is given by

$$\frac{1}{s_j} = \int_0^\infty dr f_j^2(r). \quad (\text{A.36})$$

The normalized wave function $\psi_j(r)$ behaves for $r \rightarrow \infty$ asymptotically as

$$\psi_j(r) \sim A_j e^{-\kappa_j r}, \quad A_j = \sqrt{s_j}. \quad (\text{A.37})$$

We can classify bound states as inner and outer according to whether $0 < \kappa_j < \kappa$ or $\kappa_j \geq \kappa$.

A.5 S-matrix

The S-matrix is defined relative to the free case:

$$S(k) = \frac{\mathcal{F}(-k)}{\mathcal{F}(k)} = (-1)^\ell \frac{f(-k)}{f(k)}. \quad (\text{A.38})$$

$S(k)$ is meromorphic inside the strip $-\kappa < \text{Im } k < \kappa$ and it has poles where $\mathcal{F}(k) = 0$. Further it has the properties

$$S(-k) = \frac{1}{S(k)}, \quad S^*(k) = S(-k^*), \quad S(0) = 1. \quad (\text{A.39})$$

For $0 < \text{Im } k < \kappa$, poles occur only for $k = i\kappa_j$. Thus there is a relation between inner bound states and S-matrix poles. All other poles of the S-matrix are unrelated to the bound state structure. The residue at an inner pole is given by the formula

$$S(k) \sim -i(-1)^\ell \frac{s_j}{k - i\kappa_j}, \quad k \sim i\kappa_j. \quad (\text{A.40})$$

For real k

$$S(k) = e^{2i\delta(k)}, \quad (\text{A.41})$$

where $\delta(k)$ is the phase shift. For small k

$$S(k) = \frac{A(k) - ik^{2\ell+1}B(k)}{A(k) + ik^{2\ell+1}B(k)} \sim 1 - 2ik^{2\ell+1} \frac{B_o}{A_o} + \dots \quad (\text{A.42})$$

Thus, for small k , both $S(k) - 1$ and $\delta(k)$ are $\mathcal{O}(k^{2\ell+1})$.

A.6 Levinson's theorem

One of the crucial modifications of the theory if the potential is singular occurs in Levinson's theorem [30]:

$$\delta(\infty) - \delta(0) = \int_0^\infty dk \delta'(k) = -\frac{\pi}{2}(2J + \nu - \ell). \quad (\text{A.43})$$

This is consistent with (A.26-A.27) since in the $k \rightarrow \infty$ limit the solutions approach that of the $\nu(\nu + 1)/r^2$ potential.

A.7 Inverse scattering

Starting from the completeness relation

$$\frac{2}{\pi} \int_0^\infty \frac{k^2 dk}{|f(k)|^2} \varphi(r, k) \varphi(s, k) + \sum_{j=1}^J s_j f_j(r) f_j(s) = \delta(r - s) \quad (\text{A.44})$$

and following the derivation in [11] we obtain, for the unknown $A(r, s)$, the following Marchenko equation

$$F(r, s) + A(r, s) + \int_r^\infty du A(r, u) F(u, s) = 0, \quad s \geq r. \quad (\text{A.45})$$

Here

$$F(r, s) = F_{\text{bound}}(r, s) + F_{\text{scatt}}(r, s) \quad (\text{A.46})$$

and

$$F_{\text{bound}}(r, s) = (-1)^{\ell+1} \sum_{j=1}^J s_j h_\ell(i\kappa_j r) h_\ell(i\kappa_j s), \quad (\text{A.47})$$

$$F_{\text{scatt}}(r, s) = -\frac{\sin \nu \pi}{\pi(r + s)} + \frac{(-1)^{\ell+1}}{2\pi} \int_0^\infty dk \left\{ [S(k) - 1] y(r, k) y(s, k) + [S(-k) - 1] y(r, -k) y(s, -k) + [1 - S(\infty)] e^{ik(r+s)} + [1 - S(-\infty)] e^{-ik(r+s)} \right\} \quad (\text{A.48})$$

with

$$y(r, k) = i^{\ell+1} h_\ell(kr). \quad (\text{A.49})$$

Note that for the simplest case of $\ell = 0$ and non-singular potential ($\nu = 0$) the usual formulas

$$F_{\text{bound}}(r, s) = \sum_{j=1}^J s_j e^{-\kappa_j(r+s)} \quad (\text{A.50})$$

and

$$F_{\text{scatt}}(r, s) = \frac{1}{2\pi} \int_{-\infty}^{\infty} dk [1 - S(k)] e^{ik(r+s)} \quad (\text{A.51})$$

are reproduced. For integer ν (A.48) can be rewritten as

$$F_{\text{scatt}}(r, s) = \frac{1}{2\pi} \int_{-\infty}^{\infty} dk \{ [S(k) - 1] h_{\ell}(rk) h_{\ell}(sk) + [(-1)^{\nu} - (-1)^{\ell}] e^{ik(r+s)} \}. \quad (\text{A.52})$$

If we can calculate the $F(r, s)$ function from scattering data and bound state information and can solve the Marchenko equation (A.45) for $A(r, s)$ then not only the potential can be expressed as

$$q(r) = -2 \frac{d}{dr} A(r, r), \quad U(r) = q(r) + \frac{\ell(\ell+1)}{r^2} \quad (\text{A.53})$$

but also the wave function is calculable [11]. It is given by the formula

$$f(r, k) = y(r, k) + \int_r^{\infty} du A(r, u) y(u, k). \quad (\text{A.54})$$

B Marchenko method for Bargmann-type S-matrices

In this appendix we apply the Marchenko method of inverse scattering to Bargmann-type (rational) S-matrices.

B.1 Rational S-matrices

A general rational solution of the $S(0) = 1$, $S(k)S(-k) = 1$ and $S^*(k) = S(-k^*)$ requirements is of the form

$$S(k) = \prod_{\alpha=1}^{\mathcal{N}_+} \frac{\lambda_{\alpha} - ik}{\lambda_{\alpha} + ik} \prod_{\beta=1}^{\mathcal{N}_-} \frac{\mu_{\beta} - ik}{\mu_{\beta} + ik}, \quad (\text{B.1})$$

where the parameters λ_{α} have positive real parts and they are either real or come in complex conjugate pairs. Similarly the real parts of μ_{β} are negative and they are also either real or form complex conjugate pairs. We assume, for simplicity, that they are all distinct so that the S-matrix (B.1) has simple poles only.

The residues at the poles in the upper half plane are given by

$$S(k) \sim \frac{-iR_{\alpha}}{k - i\lambda_{\alpha}} \quad k \sim i\lambda_{\alpha}, \quad (\text{B.2})$$

where

$$R_{\alpha} = 2\lambda_{\alpha} \prod_{\alpha' \neq \alpha} \frac{\lambda_{\alpha'} + \lambda_{\alpha}}{\lambda_{\alpha'} - \lambda_{\alpha}} \prod_{\beta} \frac{\mu_{\beta} + \lambda_{\alpha}}{\mu_{\beta} - \lambda_{\alpha}}. \quad (\text{B.3})$$

R_α is real for λ_α real and $R_\alpha^* = R_{\bar{\alpha}}$ for $\lambda_\alpha = \lambda_{\bar{\alpha}}^*$ complex conjugate pairs.

Given the S-matrix (B.1) we still have to specify $\{s_j, \kappa_j\}_{j=1}^J$, $s_j > 0, \kappa_j > 0$, i.e. the number of bound states and the corresponding binding energies and asymptotic decay constants. Moreover, these data have to satisfy the following constraints:

- For higher partial waves $\ell \geq 1$ the S-matrix parameters have to be chosen such that (B.1) satisfies the

$$S(k) = 1 + O(k^{2\ell+1}) \quad (\text{B.4})$$

constraint for small k .

- The singularity strength, obtained from Levinson's theorem (A.43), is given by

$$\nu = \mathcal{N}_+ - \mathcal{N}_- - 2J + \ell \quad (\text{B.5})$$

in this case and has to be a non-negative integer.

- Because of the relation between S-matrix poles and inner bound states the sets

$$\{\lambda_\alpha \mid \text{Re}(\lambda_\alpha) < \kappa\} \quad \text{and} \quad \{\kappa_j < \kappa\} \quad (\text{B.6})$$

must coincide, moreover, the corresponding residues (for $\lambda_\alpha = \kappa_j$) are restricted by $R_\alpha = (-1)^\ell s_j$, which is possible only if

$$(-1)^\ell R_\alpha > 0. \quad (\text{B.7})$$

The advantage of using rational S-matrices is that the singularity strength ν is always an integer and when calculating the scattering contribution to Marchenko's F function we can use (A.52), which is now easily evaluated using Cauchy's theorem by closing the contour in the upper half plane:

$$F_{\text{scatt}}(r, s) = \sum_\alpha R_\alpha h_\ell(i\lambda_\alpha r) h_\ell(i\lambda_\alpha s). \quad (\text{B.8})$$

The contributions coming from the terms with $\text{Re}(\lambda_\alpha) < \kappa$ are canceled by the same, but opposite sign contributions of the inner bound states to F_{bound} , so the final result for the full F function is given by

$$F(r, s) = \sum_{\text{Re}(\lambda_\alpha) \geq \kappa} R_\alpha h_\ell(i\lambda_\alpha r) h_\ell(i\lambda_\alpha s) + (-1)^{\ell+1} \sum_{\kappa_j \geq \kappa} s_j h_\ell(i\kappa_j r) h_\ell(i\kappa_j s). \quad (\text{B.9})$$

Since the form of these remaining terms are the same, we can combine them and write

$$F(r, s) = \sum_{n=1}^N R_n h_\ell(ig_n r) h_\ell(ig_n s), \quad \text{Re}(g_n) > 0, \quad (\text{B.10})$$

where the parameters g_n are either real or come in complex conjugate pairs and the coefficient R_n is real for real g_n and $R_n^* = R_{\bar{n}}$ for complex conjugate pairs.

B.2 Algebraic equation

For rational S-matrices the solution of the Marchenko integral equation is completely algebraic [19, 20]. We have simplified the derivation and expressed the final result in a compact form.

Let us introduce the shorthand notation $\omega_n(r) = h_\ell(ig_n r)$. Then the Marchenko integral equation with $F(r, s)$ given by (B.10) becomes

$$\sum_{n=1}^N R_n \omega_n(r) \omega_n(s) + A(r, s) + \sum_{n=1}^N R_n \omega_n(s) \int_r^\infty du A(r, u) \omega_n(u) = 0. \quad (\text{B.11})$$

Thus the solution for $A(r, s)$ has to be of the form

$$A(r, s) = - \sum_{n=1}^N b_n(r) \omega_n(s), \quad (\text{B.12})$$

where

$$\begin{aligned} b_n(r) &= R_n \omega_n(r) + R_n \int_r^\infty du A(r, u) \omega_n(u) \\ &= R_n \omega_n(r) - R_n \sum_{m=1}^N b_m(r) \int_r^\infty \omega_n(u) \omega_m(u) du. \end{aligned} \quad (\text{B.13})$$

The second equality is a linear algebraic set of equations for the unknown coefficients $b_n(r)$:

$$\frac{1}{R_n} b_n(r) + \sum_{m=1}^N I_{nm}(r) b_m(r) = \omega_n(r), \quad (\text{B.14})$$

where

$$I_{nm}(r) = \int_r^\infty \omega_n(u) \omega_m(u) du = \int_r^\infty h_\ell(ig_n u) h_\ell(ig_m u) du. \quad (\text{B.15})$$

Using the properties of the Hankel functions, the integral of the product of two Hankel functions can be done in terms of other Hankel functions[†]:

$$I_{nm}(r) = \frac{i}{g_n^2 - g_m^2} \{ g_m h_\ell(ig_n r) h_{\ell-1}(ig_m r) - g_n h_\ell(ig_m r) h_{\ell-1}(ig_n r) \} \quad (\text{B.16})$$

for $n \neq m$ and

$$I_{nn}(r) = \frac{r}{2} \{ h_{\ell-1}(ig_n r) h_{\ell+1}(ig_n r) - h_\ell^2(ig_n r) \}. \quad (\text{B.17})$$

[†]We define $h_{-1}(x) = e^{ix}$.

Introducing the matrix of the linear problem,

$$\mathcal{M}_{nm}(r) = \frac{1}{R_n} \delta_{nm} + I_{nm}(r), \quad (\text{B.18})$$

we have to solve

$$\sum_{m=1}^N \mathcal{M}_{nm}(r) b_m(r) = \omega_n(r). \quad (\text{B.19})$$

The solution is

$$b_n(r) = \sum_{m=1}^N \mathcal{N}_{nm}(r) \omega_m(r), \quad (\text{B.20})$$

where \mathcal{N} is the matrix inverse of \mathcal{M} . To calculate the potential we only need

$$A(r, r) = - \sum_{n=1}^N b_n(r) \omega_n(r) = - \sum_{n,m=1}^N \omega_n(r) \mathcal{N}_{nm}(r) \omega_m(r), \quad (\text{B.21})$$

which can also be written as

$$A(r, r) = \sum_{n,m=1}^N \mathcal{N}_{nm}(r) \frac{d}{dr} \mathcal{M}_{mn}(r) = \text{Tr}[\mathcal{M}^{-1} \frac{d}{dr} \mathcal{M}(r)] = \frac{d}{dr} \ln \det(\mathcal{M}). \quad (\text{B.22})$$

The final result is

$$q(r) = -2 \frac{d^2}{dr^2} \ln \det(\mathcal{M}). \quad (\text{B.23})$$

B.3 s-wave scattering

The formulas simplify in the case of s-wave scattering ($\ell = 0$). In this case the Hankel functions become simple exponentials and Marchenko's F takes the form

$$F(r, s) = F(x) = - \sum_{m=1}^N R_m e^{-\omega_m x}, \quad x = r + s. \quad (\text{B.24})$$

To express the solution in simple terms it is useful to define

$$\mathcal{K}_{mn} = \frac{1}{z_m} \delta_{mn} - \frac{1}{\omega_m + \omega_n}, \quad z_m(r) = R_m e^{-2\omega_m r}. \quad (\text{B.25})$$

Then

$$q(r) = -2 \frac{d}{dr} A(r, r) = -2 \frac{d^2}{dr^2} \ln |\det(\mathcal{K})| \quad (\text{B.26})$$

and the bound state wave functions can also be calculated algebraically:

$$f_j(r) = e^{-\kappa_j r} \left\{ 1 + \sum_{m=1}^N \frac{\gamma_m(r)}{\kappa_j + \omega_m} \right\}, \quad (\text{B.27})$$

where

$$\gamma_m = \sum_{k=1}^N (\mathcal{K}^{-1})_{mk}. \quad (\text{B.28})$$

B.4 Examples

In this subsection and the next we will discuss examples most of which we used in the main text. All our examples correspond to s-wave scattering ($\ell = 0$). We will use the $(\mathcal{N}_+, \mathcal{N}_-)[J]$ notation and first consider the $(3, 0)[1]$ case. In this case

$$S(k) = \sigma_a(k)\sigma_b(k)\sigma_c(k), \quad a, b, c > 0. \quad (\text{B.29})$$

We define the constants

$$\tilde{R}_a = 2a \frac{(b+a)(c+a)}{(b-a)(c-a)}, \quad \tilde{R}_b = 2b \frac{(a+b)(c+b)}{(a-b)(c-b)}, \quad \tilde{R}_c = 2c \frac{(a+c)(b+c)}{(a-c)(b-c)} \quad (\text{B.30})$$

We will assume that the single bound state coincides with one of the parameters, $\kappa_o = b$. The corresponding norming constant can be parametrized as $s_o = y\tilde{R}_b$ and we write

$$F(r) = (y-1)\tilde{R}_b e^{-br} - \tilde{R}_a e^{-ar} - \tilde{R}_c e^{-cr}. \quad (\text{B.31})$$

We will study two cases: $y = 1$ and $y = 2$. These are only possible if b is the smallest (or largest) parameter of the S-matrix since the norming constant must be positive. The first choice corresponds to treating $k = ib$ as inner pole, in which case this term is eliminated from $F(r)$ completely. The second one can be called the sign-flip choice.

In the first case where $y = 1$ and $N = 2$ we have

$$\omega_1 = a, \quad \omega_2 = c, \quad R_1 = \tilde{R}_a, \quad R_2 = \tilde{R}_c. \quad (\text{B.32})$$

Therefore, this is a 2×2 matrix problem with

$$\mathcal{K}_1 = \begin{pmatrix} \frac{e^{2ar}}{\tilde{R}_a} - \frac{1}{2a} & -\frac{1}{a+c} \\ -\frac{1}{a+c} & \frac{e^{2cr}}{\tilde{R}_c} - \frac{1}{2c} \end{pmatrix} \quad (\text{B.33})$$

and can easily be solved explicitly for general a, b, c . The solution is given in sect. 3.1.

In the sign-flip case $N = 3$ and

$$\omega_1 = b, \quad \omega_2 = a, \quad \omega_3 = c, \quad R_1 = -\tilde{R}_b, \quad R_2 = \tilde{R}_a, \quad R_3 = \tilde{R}_c. \quad (\text{B.34})$$

Furthermore we take $b = 1$, $a = 2$ and $c = 4$. The corresponding 3×3 matrix is

$$\mathcal{K}_2 = \begin{pmatrix} -\frac{1}{10}e^{2r} - \frac{1}{2} & -\frac{1}{3} & -\frac{1}{5} \\ -\frac{1}{3} & -\frac{1}{36}e^{4r} - \frac{1}{4} & -\frac{1}{6} \\ -\frac{1}{5} & -\frac{1}{6} & \frac{1}{40}e^{8r} - \frac{1}{8} \end{pmatrix}. \quad (\text{B.35})$$

From (B.26) and (B.27) we get

$$q(r) = \frac{2}{\sinh^2 r} - \frac{12}{\cosh^2 r} \quad (\text{B.36})$$

and

$$f_o(r) = \frac{1}{2} \frac{\sinh^2 r}{\cosh^3 r} = \frac{1}{2} \varphi_o(r). \quad (\text{B.37})$$

These are the generalized Pöschl-Teller (PT) potential and its ground state wave function [31].

B.5 More examples

Let us consider more examples. Firstly, we investigate the $(4, 0)[1]$ case where the scattering matrix is represented as

$$S(k) = \sigma_a(k)\sigma_b(k)\sigma_c(k)\sigma_d(k). \quad (\text{B.38})$$

Without going any further, we observe that $S(k)$ falls into the class of PT type potentials with the degree of singularity $\nu = 2$ according to Levinson's theorem.

As before, we identify the bound state momentum κ_o with b . We find

$$F(r) = (y - 1)\tilde{R}_b e^{-br} - \tilde{R}_a e^{-ar} - \tilde{R}_c e^{-cr} - \tilde{R}_d e^{-dr}, \quad (\text{B.39})$$

where the \tilde{R}_m -s read

$$\begin{aligned} \tilde{R}_a &= -2a \frac{(a+b)(a+c)(a+d)}{(a-b)(a-c)(a-d)}, & \tilde{R}_b &= -2b \frac{(b+a)(b+c)(b+d)}{(b-a)(b-c)(b-d)}, \\ \tilde{R}_c &= -2c \frac{(c+a)(c+b)(c+d)}{(c-a)(c-b)(c-d)}, & \tilde{R}_d &= -2d \frac{(d+a)(d+b)(d+c)}{(d-a)(d-b)(d-c)}. \end{aligned} \quad (\text{B.40})$$

In subsection 3.2 we used the complex parameters of Ref. [15]. We note that this choice of the parameters yields, once more, a real and positive \tilde{R}_b . Therefore, we are able to cancel it by choosing $y = 1$. We are left with

$$\omega_1 = a, \quad \omega_2 = c, \quad \omega_3 = d, \quad R_1 = \tilde{R}_a, \quad R_2 = \tilde{R}_c, \quad R_3 = \tilde{R}_d. \quad (\text{B.41})$$

The corresponding potential is shown in Fig. 3b (section 3).

Finally, we consider a $(4, 1)[1]$ type S-matrix composed of 5 factors

$$S(k) = \sigma_a(k)\sigma_b(k)\sigma_c(k)\sigma_d(k)\sigma_e(k), \quad (\text{B.42})$$

with one of its poles (a) being negative [18]. Once again, the bound state momentum is $\kappa_o = b$. Since the contour is closed in upper half plane, the negative pole does not contribute to the integral (A.51). Therefore we obtain

$$F(r) = (y - 1)\tilde{R}_b e^{-br} - \tilde{R}_c e^{-cr} - \tilde{R}_d e^{-dr} - \tilde{R}_e e^{-er}, \quad (\text{B.43})$$

where

$$\begin{aligned} \tilde{R}_b &= 2b \frac{(b+a)(b+c)(b+d)(b+e)}{(b-a)(b-c)(b-d)(b-e)}, & \tilde{R}_c &= 2c \frac{(c+a)(c+b)(c+d)(c+e)}{(c-a)(c-b)(c-d)(c-e)}, \\ \tilde{R}_d &= 2d \frac{(d+a)(d+b)(d+c)(d+e)}{(d-a)(d-b)(d-c)(d-e)}, & \tilde{R}_e &= 2e \frac{(e+a)(e+b)(e+c)(e+d)}{(e-a)(e-b)(e-c)(e-d)}. \end{aligned} \quad (\text{B.44})$$

We again focus on the $y = 1$ case and write

$$\omega_1 = c, \quad \omega_2 = d, \quad \omega_3 = e, \quad R_1 = \tilde{R}_c, \quad R_2 = \tilde{R}_d, \quad R_3 = \tilde{R}_e. \quad (\text{B.45})$$

The corresponding potential is shown in Fig. 3c (section 3).

C Coupled channel problems

For coupled channel problems different partial waves $\psi_a(r)$ $a = 1, \dots, N$ (with orbital angular momentum ℓ_a) are mixed by the potential term in the radial Schrödinger equation:

$$-\frac{\hbar^2}{2m}\psi_a''(r) + \sum_{b=1}^N U_{ab}(r)\psi_b(r) + \frac{\hbar^2}{2m}\frac{\ell_a(\ell_a+1)}{r^2}\psi_a(r) = E\psi_a(r), \quad (\text{C.1})$$

where m is the reduced mass of the system. We will assume that the potential matrix U_{ab} is real and symmetric. In the case of nucleon scattering it is usually assumed that in addition to the total angular momentum j the total spin S is also conserved, so in this application spin triplet ($S = 1$) scattering is a coupled channel problem with $N = 2$ and $\ell_{1,2} = j \mp 1$.

After rescaling

$$U_{ab}(r) = \frac{\hbar^2}{2m}q_{ab}(r), \quad E = \frac{\hbar^2 k^2}{2m} \quad (\text{C.2})$$

the Schrödinger equation becomes

$$-\psi_a''(r) + V_{ab}(r)\psi_b(r) = k^2\psi_a(r) \quad (\text{C.3})$$

with

$$V_{ab}(r) = q_{ab}(r) + \frac{\ell_a(\ell_a+1)}{r^2}\delta_{ab}. \quad (\text{C.4})$$

The details of scattering and inverse scattering theory depend on the class of potentials. Here we will consider the case of real symmetric potentials with asymptotic behaviour

$$q_{ab}(r) \sim \frac{\beta_{ab}}{r^2} + O(1), \quad r \rightarrow 0, \quad \beta_{ab} = \beta_{ba} \quad \text{real}, \quad (\text{C.5})$$

$$q_{ab}(r) \sim e^{-2\kappa r}, \quad r \rightarrow \infty, \quad (\kappa > 0). \quad (\text{C.6})$$

For the total potential term in the radial Schrödinger equation this implies

$$V_{ab}(r) \sim \frac{\nu_{ab}}{r^2} + O(1), \quad r \rightarrow 0, \quad \nu_{ab} = \beta_{ab} + \ell_a(\ell_a + 1)\delta_{ab}, \quad (\text{C.7})$$

$$V_{ab}(r) \sim \frac{\ell_a(\ell_a + 1)}{r^2} \delta_{ab} + \text{exp. small}, \quad r \rightarrow \infty. \quad (\text{C.8})$$

C.1 Regular solutions, Jost solutions, Jost functions

Apart from obvious complications related to the multi-component nature of the coupled problem the scattering and inverse scattering theory is very similar to the single channel case discussed in appendix A so here we can be brief.

The Wronskian $W[\rho, \sigma]$ of two vectors $\rho \sim \rho_a(r)$ and $\sigma \sim \sigma_a(r)$ is defined as

$$(W[\rho, \sigma])(r) = \rho'_a(r)\sigma_a(r) - \rho_a(r)\sigma'_a(r). \quad (\text{C.9})$$

It is constant if ρ and σ are both solutions of the Schrödinger equation with the same k^2 .

The Schrödinger equation (C.3) is written in the basis of partial waves corresponding to fixed values of the orbital angular momentum ℓ_a . The total potential matrix V_{ab} is diagonal in this basis for asymptotically large distances. An other basis can be obtained by diagonalizing the potential for $r \rightarrow 0$:

$$\nu_{ab} = \sum_{A=1}^N \omega_{aA} \omega_{bA} \nu_A (\nu_A + 1) \quad (\text{C.10})$$

with a real, orthogonal matrix ω_{aA} satisfying $\omega_{aA} \omega_{bA} = \delta_{ab}$. We are interested in the case of repulsive potentials so we will assume that the eigenvalues are positive: $\nu_A \geq 0$, $A = 1, \dots, N$.

The N regular solutions $\varphi_k^A = \varphi^A(k)$ $A = 1, \dots, N$ are non-singular for small r and have simple behaviour in this basis:

$$(\varphi_k^A)_a(r) \sim \omega_{aA} r^{\nu_A + 1} \quad r \rightarrow 0 \quad (\text{C.11})$$

and they are well-defined and analytic for all k satisfying

$$\varphi^A(-k) = \varphi^A(k), \quad [\varphi^A(k)]^* = \varphi^A(k^*). \quad (\text{C.12})$$

The N Jost solutions $f_k^\alpha = f^\alpha(k)$ $\alpha = 1, \dots, N$ are defined by their asymptotic behaviour for large r :

$$(f_k^\alpha)_a(r) \sim \delta_a^\alpha e^{ikr}, \quad r \rightarrow \infty \quad (\text{C.13})$$

and are well defined for $\text{Im } k \geq 0$ ($k \neq 0$) and analytic for $k > 0$. Moreover

$$[f^\alpha(k)]^* = f^\alpha(-k^*). \quad (\text{C.14})$$

The *Jost function (matrix)* is defined here as

$$f^{A\alpha}(k) = W[\varphi^A(k), f^\alpha(k)], \quad A, \alpha = 1, \dots, N. \quad (\text{C.15})$$

It is also analytic in the upper half-plane ($k > 0$), well defined for all $\text{Im } k \geq 0$ ($k \neq 0$) and satisfies

$$[f^{A\alpha}(k)]^* = f^{A\alpha}(-k^*). \quad (\text{C.16})$$

Its matrix inverse

$$g(k) = f^{-1}(k), \quad g^{\beta A}(k) f^{A\alpha}(k) = \delta^{\alpha\beta} \quad (\text{C.17})$$

has similar properties. The large distance asymptotics of the solution ($k \neq 0$ real)

$$g^{\beta A}(k) \varphi_k^A = \frac{i}{2k} \left\{ f_{-k}^\beta - g^{\beta A}(k) f^{A\alpha}(-k) f_k^\alpha \right\} \quad (\text{C.18})$$

reveals that it is a superposition of an incoming free wave and an outgoing wave:

$$r \rightarrow \infty : \quad \frac{i}{2k} \left\{ \delta_a^\beta e^{-ikr} - \sigma^{\beta a}(k) e^{ikr} \right\} \quad (\text{C.19})$$

with scattering matrix

$$\sigma^{\alpha\beta}(k) = g^{\alpha A}(k) f^{A\beta}(-k), \quad \sigma(k) = f^{-1}(k) f(-k). \quad (\text{C.20})$$

It can be shown that $\sigma(k)$ has the properties

$$\sigma^*(k) = \sigma(-k), \quad \sigma^T(k) = \sigma(k), \quad \sigma(k) \sigma(-k) = 1, \quad (\text{C.21})$$

so it is a symmetric unitary matrix.

Similarly to the single channel Jost solution, f_k^α also satisfies an integral equation which allows an analytic extension on the complex k plane beyond the original domain of definition (the upper half-plane). The rescaled Jost function

$$\mathcal{F}_k^\alpha = (-ik)^{\ell_\alpha} f_k^\alpha \quad (\text{C.22})$$

is analytic for $\text{Im } k > -\kappa$ (including $k = 0$). This implies that $\sigma(k)$ is meromorphic in the strip $|\text{Im } k| < \kappa$.

C.2 The physical S-matrix

The physical S-matrix is defined relative to the free (no potential) case:

$$S(k) = i^L \sigma(k) i^L, \quad (\text{C.23})$$

where $L = \text{diag}(\ell_1, \dots, \ell_N)$. We assume that all ℓ_a are of the same parity: $(-1)^L = \pm 1$. In this case the physical S-matrix $S(k)$ is also symmetric unitary for real k , meromorphic in the above strip and satisfies there

$$S^T(k) = S(k), \quad S^*(k) = S(-k^*), \quad S(k)S(-k) = 1. \quad (\text{C.24})$$

In addition, if there are no zero energy bounded solutions, which we assume, for small k it can be expanded as

$$S^{\alpha\beta}(k) = \delta^{\alpha\beta} + O(k^{\ell_\alpha + \ell_\beta + 1}). \quad (\text{C.25})$$

Physical phase shifts can be found by diagonalizing the S-matrix for real k as

$$S^{\alpha\beta}(k) = \sum_{A=1}^N O_{\alpha A}(k) O_{\beta A}(k) e^{2i\delta_A(k)}, \quad (\text{C.26})$$

where $O_{\alpha A}(k)$ is a real orthogonal matrix, symmetric in k and the phase shifts $\delta_A(k)$ $A = 1, \dots, N$ are odd functions of k (modulo π).

C.3 Bound states

If for some $k = k_o$ the Jost function matrix is singular, $\det f(k_o) = 0$, then some linear combination of the regular solutions $\varphi_{k_o}^A$ are also linear combination of the Jost solutions $f_{k_o}^\alpha$. This linear combination is integrable both at $r = 0$ and at $r \rightarrow \infty$ and hence a genuine eigenvector of the Hamiltonian with eigenvalue k_o^2 . Since this is impossible for real k_o and the Hamiltonian is hermitean with real eigenvalues, the only possibility is that k_o is imaginary. The set of solutions

$$k_o = i\kappa_j, \quad j = 1, \dots, J \quad (\text{C.27})$$

correspond to normalizable bound states. We will assume that there is a unique (up to normalization) solution for each κ_j :

$$f_a^{(j)}(r) = v_{(j)}^\alpha (f_{i\kappa_j}^\alpha)_a(r), \quad \sum_\alpha (v_{(j)}^\alpha)^2 = 1. \quad (\text{C.28})$$

This solution, and the linear combination coefficients $v_{(j)}^\alpha$ are real. We can find the normalized bound state wave function

$$\psi_a^{(j)}(r) = w_{(j)}^\alpha (f_{i\kappa_j}^\alpha)_a(r) \quad (\text{C.29})$$

by calculating the norming constants

$$\frac{1}{s_j} = \sum_{a=1}^N \int_0^\infty (f_a^{(j)}(r))^2 dr \quad (C.30)$$

and putting $w_{(j)}^\alpha = \sqrt{s_j} v_{(j)}^\alpha$.

Like in the single channel case, we can distinguish inner and outer bound states according to whether $\kappa_j < \kappa$ or $\kappa_j \geq \kappa$, respectively. For inner bound states only, the corresponding pole of the scattering matrix is related to the bound state properties:

$$\sigma^{\alpha\beta}(k) \sim \frac{-i w_{(j)}^\alpha w_{(j)}^\beta}{k - i\kappa_j}, \quad (\text{near } k = i\kappa_j). \quad (C.31)$$

C.4 Marchenko equation

The derivation of Marchenko's equation for the coupled channel case proceeds along the same line as for the single channel problem. The main difference is that here a set of linear equations

$$F_{ab}(r, s) + A_{ab}(r, s) + \int_r^\infty A_{ac}(r, u) F_{cb}(u, s) du = 0, \quad s \geq r \quad (C.32)$$

has to be solved for the unknowns $A_{ab}(r, s)$, where

$$F_{cd}(u, v) = F_{cd}^{\text{bound}}(u, v) + F_{cd}^{\text{scatt}}(u, v) \quad (C.33)$$

with

$$F_{cd}^{\text{bound}}(u, v) = \sum_{j=1}^J w_{(j)}^\alpha w_{(j)}^\beta y_c^\alpha(i\kappa_j u) y_d^\beta(i\kappa_j v), \quad (C.34)$$

$$\begin{aligned} F_{cd}^{\text{scatt}}(u, v) &= \frac{1}{2\pi i(u+v)} [\sigma^{cd}(\infty) - \sigma^{cd}(-\infty)] \\ &+ \frac{1}{2\pi} \int_0^\infty dk \{ [(-1)^L \delta^{\alpha\beta} - \sigma^{\alpha\beta}(k)] y_c^\alpha(ku) y_d^\beta(kv) \\ &\quad + [(-1)^L \delta^{\alpha\beta} - \sigma^{\alpha\beta}(-k)] y_c^\alpha(-ku) y_d^\beta(-kv) \\ &\quad + [\sigma^{cd}(\infty) - (-1)^L \delta_{cd}] e^{ik(u+v)} + [\sigma^{cd}(-\infty) - (-1)^L \delta_{cd}] e^{-ik(u+v)} \}. \end{aligned} \quad (C.35)$$

In the above formulas

$$y_a^\alpha(x) = (i)^{\ell_\alpha+1} h_{\ell_\alpha}(x) \delta_a^\alpha. \quad (C.36)$$

The infinite momentum scattering matrices are calculated to be

$$\sigma^{\alpha\beta}(\infty) = \sum_{A=1}^N \omega_{\alpha A} \omega_{\beta A} e^{-i\pi\nu_A}, \quad \sigma^{\alpha\beta}(-\infty) = \sum_{A=1}^N \omega_{\alpha A} \omega_{\beta A} e^{i\pi\nu_A}. \quad (C.37)$$

These are generalizations of (A.27).

If (and only if) all ν_A eigenvalues are integer then $\sigma(\infty) = \sigma(-\infty)$ and this allows to simplify (C.34-C.35) as follows.

$$F_{cd}^{\text{bound}}(u, v) = (-1)^{\frac{\ell_c + \ell_d}{2} + 1} \sum_{j=1}^J w_{(j)}^c w_{(j)}^d h_{\ell_c}(i\kappa_j u) h_{\ell_d}(i\kappa_j v), \quad (\text{C.38})$$

$$\begin{aligned} F_{cd}^{\text{scatt}}(u, v) &= \frac{1}{2\pi} \int_{-\infty}^{\infty} dk \{ [S^{cd}(k) - \delta_{cd}] h_{\ell_c}(ku) h_{\ell_d}(kv) \\ &\quad + \sum_{A=1}^N \omega_{cA} \omega_{dA} [(-1)^{\nu_A} - (-1)^L] e^{ik(u+v)} \}. \end{aligned} \quad (\text{C.39})$$

C.5 Levinson's theorem

The derivation [30] of Levinson's theorem can be generalized to give

$$\int_0^{\infty} dk \text{Tr}\{S^{-1}(k)S'(k)\} = 2i \sum_{A=1}^N \int_0^{\infty} \delta'_A(k) dk, \quad (\text{C.40})$$

but this only allows us to write one “total” Levinson's theorem

$$-\frac{2}{\pi} \sum_{A=1}^N \int_0^{\infty} \delta'_A(k) dk = \frac{2}{\pi} \sum_{A=1}^N [\delta_A(0) - \delta_A(\infty)] = 2J + \sum_{A=1}^N \nu_A - \sum_{a=1}^N \ell_a. \quad (\text{C.41})$$

From (C.37) one can conclude that there are also “individual” Levinson's type formulas

$$\delta_A(\infty) = -\frac{\pi}{2} \nu_A, \quad A = 1, \dots, N, \quad (\text{C.42})$$

but these are valid only modulo π .

C.6 Inverse scattering with Marchenko's method

Inverse scattering is a method to calculate the potential matrix $q_{ab}(r)$ from the scattering data

$$\mathcal{S} = \{L; S^{ab}(k), -\infty < k < \infty; \{w_{(j)}^a, \kappa_j\}_{j=1}^J\}. \quad (\text{C.43})$$

The S-matrix has to be regular and its analytic extension to the strip $|\text{Im}k| < \kappa$ has to be a meromorphic function satisfying the symmetry relations (C.24). Its expansion around the origin is constrained by (C.25), moreover after finding the eigenshifts by the decomposition (C.26) the Levinson's theorem (C.41) must be satisfied by

nonnegative ν_A parameters. In the strip $0 < \text{Im}k < \kappa$ $S^{ab}(k)$ can have simple poles only at $k = i\kappa_j$, for all the inner poles, with residue

$$-i(-1)^{\frac{\ell_a+\ell_b}{2}} w_{(j)}^a w_{(j)}^b. \quad (\text{C.44})$$

The first step of the inverse scattering procedure is the calculation of Marchenko's F -functions from the scattering data by (C.33, C.34, C.35). The second step is the solution of the set of linear integral equations (C.32) to find $A_{ab}(u, v)$.

The third and final step is to calculate the potential using the formula

$$V_{ab}(r) = \frac{\ell_a(\ell_a + 1)}{r^2} \delta_{ab} - 2 \frac{d}{dr} A_{ab}(r, r). \quad (\text{C.45})$$

The wave functions can be obtained by the mapping

$$(f_k^\alpha)_a(r) = y_a^\alpha(kr) + \int_r^\infty A_{ab}(r, s) y_b^\alpha(ks) ds. \quad (\text{C.46})$$

C.7 $N = 2$ parametrization

For applications to nucleon scattering we need the special case $N = 2$. In this case a useful parametrization is given by

$$S(k) = \frac{A(k) + B(k)}{2} + \frac{(A(k) - B(k))z(k)}{4} \rho_+ + \frac{A(k) - B(k)}{4z(k)} \rho_-, \quad (\text{C.47})$$

where

$$\rho_\pm = \begin{pmatrix} 1 & \pm i \\ \pm i & -1 \end{pmatrix}. \quad (\text{C.48})$$

The symmetry of the S-matrix is already built in and the other two requirements in (C.24) are satisfied if

$$\left. \begin{aligned} A(k)A(-k) &= 1 \\ A^*(k)A(k^*) &= 1 \end{aligned} \right\}, \quad \left. \begin{aligned} B(k)B(-k) &= 1 \\ B^*(k)B(k^*) &= 1 \end{aligned} \right\}, \quad \left. \begin{aligned} z(k) &= z(-k) \\ z^*(k)z(k^*) &= 1 \end{aligned} \right\}. \quad (\text{C.49})$$

$A(k)$ and $B(k)$ are exactly like the scalar S-'matrix' in a single channel problem, but the mixing part $z(k)$ is different. For real k , $\delta_{1,2}(k)$ is odd in k (modulo π) and $\epsilon(k)$ is even (also modulo π). This parametrization is the same as (4.1-4.2) after the identification

$$A(k) = e^{2i\delta_1(k)}, \quad B(k) = e^{2i\delta_2(k)}, \quad z(k) = e^{-2i\epsilon(k)}. \quad (\text{C.50})$$

Note that the $k \rightarrow 0$ constraint (C.25) and the residue constraint (C.44) still need to be imposed.

C.8 Rational S-matrix

In this paper we work with rational S-matrices only so in this subsection we apply the general theory to this special case. Rational S-matrices are automatically meromorphic for all k and satisfy

$$S(\infty) = S(-\infty) = S_\infty. \quad (\text{C.51})$$

If we assume (for simplicity) that all poles are simple then the S-matrix can be written algebraically as

$$S^{ab}(k) = S_\infty^{ab} + \sum_n \frac{-iR_n^{ab}}{k - i\eta_n}, \quad R_n^{ab} = R_n^{ba}. \quad (\text{C.52})$$

The pole parameters η_n are either real or come in complex conjugate pairs: $\eta_n^* = \eta_{\bar{n}}$ and also the residues satisfy $(R_n^{ab})^* = R_{\bar{n}}^{ab}$.

Let the set of inner bound states be $\{\kappa_j\}$, $j = 1, \dots, J_o$. Then the set of pole parameters can be classified as

$$\{\eta_n\} = \{\kappa_j\}_{j=1}^{J_o} \cup \{\lambda_\alpha\} \cup \{\mu_\beta\}, \quad (\text{C.53})$$

where $\text{Re}(\lambda_\alpha) > \kappa_{J_o}$, $\text{Re}(\mu_\beta) < 0$ and correspondingly

$$S^{ab}(k) = S_\infty^{ab} + \sum_{j=1}^{J_o} \frac{-iR_{(j)}^{ab}}{k - i\kappa_j} + \sum_\alpha \frac{-iR_\alpha^{ab}}{k - i\lambda_\alpha} + \sum_\beta \frac{-i\tilde{R}_\beta^{ab}}{k - i\mu_\beta}, \quad (\text{C.54})$$

where

$$R_{(j)}^{ab} = (-1)^{\frac{\ell_a + \ell_b}{2}} w_{(j)}^a w_{(j)}^b. \quad (\text{C.55})$$

From (C.38) we get

$$F_{cd}^{\text{bound}}(u, v) = - \sum_{j=1}^J R_{(j)}^{cd} h_{\ell_c}(i\kappa_j u) h_{\ell_d}(i\kappa_j v) \quad (\text{C.56})$$

and from (C.39), doing the integral after closing the contour in the upper half-plane,

$$F_{cd}^{\text{scatt}}(u, v) = \sum_{j=1}^{J_o} R_{(j)}^{cd} h_{\ell_c}(i\kappa_j u) h_{\ell_d}(i\kappa_j v) + \sum_\alpha R_\alpha^{cd} h_{\ell_c}(i\lambda_\alpha u) h_{\ell_d}(i\lambda_\alpha v). \quad (\text{C.57})$$

We see that the contribution of the inner poles completely cancels. The final result for Marchenko's F -function takes the form

$$F_{cd}(u, v) = \sum_m R_m^{cd} h_{\ell_c}(i\xi_m u) h_{\ell_d}(i\xi_m v), \quad (\text{C.58})$$

where the set of relevant poles is

$$\{\xi_m\} = \{\kappa_j\}_{j=J_o+1}^J \cup \{\lambda_\alpha\}. \quad (\text{C.59})$$

C.9 Algebraic solution

The advantage of using Marchenko's method for rational S-matrices is that the solution can be obtained algebraically [19, 20]. Introducing the notation

$$\omega_n^{(a)}(r) = h_{\ell_a}(i\xi_n r) \quad (\text{C.60})$$

(C.58) reads

$$F_{cd}(u, v) = \sum_n R_n^{cd} \omega_n^{(c)}(u) \omega_n^{(d)}(v). \quad (\text{C.61})$$

From the Marchenko equation (C.32) we first obtain that the solution must be of the form

$$A_{ab}(r, s) = - \sum_n \mathcal{V}_n^{ab}(r) \omega_n^{(b)}(s) \quad (\text{C.62})$$

and then the equation can be reduced to a set of linear algebraic equations for the unknowns $\mathcal{V}_n^{ab}(r)$:

$$\sum_{m,c} \mathcal{V}_m^{ac}(r) \mathcal{M}_{mn}^{cb}(r) = \omega_n^{(a)}(r) R_n^{cb}. \quad (\text{C.63})$$

The matrix of the linear problem is

$$\mathcal{M}_{mn}^{cb}(r) = \delta^{cb} \delta_{mn} + I_{mn}^{(c)}(r) R_n^{cb}, \quad (\text{C.64})$$

where

$$I_{mn}^{(c)}(r) = \int_r^\infty du \omega_m^{(c)}(u) \omega_n^{(c)}(u). \quad (\text{C.65})$$

This integral can be explicitly evaluated using (B.16-B.17).

Introducing the matrix inverse $\mathcal{N}_{nk}^{bd}(r)$ satisfying

$$\sum_{n,b} \mathcal{M}_{mn}^{cb}(r) \mathcal{N}_{nk}^{bd}(r) = \delta^{cd} \delta_{mk} \quad (\text{C.66})$$

the solution for $\mathcal{V}_k^{ad}(r)$ is

$$\mathcal{V}_k^{ad}(r) = \sum_{n,b} \omega_n^{(a)}(r) R_n^{ab} \mathcal{N}_{nk}^{bd}(r) \quad (\text{C.67})$$

and finally we obtain

$$A_{ab}(r, s) = - \sum_{n,k,c} \omega_n^{(a)}(r) R_n^{ac} \mathcal{N}_{nk}^{cb}(r) \omega_k^{(b)}(s). \quad (\text{C.68})$$

References

- [1] V. G. J. Stoks, R. A. M. Klomp, C. P. F. Terheggen and J. J. de Swart, Phys. Rev. C **49**, 2950 (1994).
- [2] R. B. Wiringa, V. G. J. Stoks and R. Schiavilla, Phys. Rev. C **51**, 38 (1995).
- [3] R. Machleidt, Phys. Rev. C **63**, 024001 (2001).
- [4] R. Machleidt and D. R. Entem, *Chiral effective field theory and nuclear forces*, Phys. Rept. **503** (2011) 1 [arXiv:1105.2919 [nucl-th]].
- [5] N. Ishii, S. Aoki and T. Hatsuda, *The nuclear force from lattice QCD*, Phys. Rev. Lett. **99**, 022001 (2007) [arXiv:nucl-th/0611096].
- [6] S. Aoki, *Hadron Interactions from lattice QCD*, EPJ Web Conf. **113** (2016) 01009 [arXiv:1603.00989 [hep-lat]].
- [7] S. Aoki, J. Balog and P. Weisz, *The Repulsive core of the NN potential and the operator product expansion*, PoS LAT **2009** (2009) 132 [arXiv:0910.4255 [hep-lat]].
- [8] S. Aoki, J. Balog and P. Weisz, *Application of the operator product expansion to the short distance behavior of nuclear potentials*, JHEP **1005** (2010) 008 [arXiv:1002.0977 [hep-lat]].
- [9] Y. Kim, S. Lee and P. Yi, *Holographic Deuteron and Nucleon-Nucleon Potential*, JHEP **0904** (2009) 086 [arXiv:0902.4048 [hep-th]].
- [10] V. A. Marchenko, *Sturm-Liouville operators and applications*, Birkhäuser, Basel, 1986.
- [11] For a review see A. G. Ramm, *One-dimensional inverse scattering and spectral problems*, CUBO a Math. Journal **6** (2004) 313-426 [arXiv:math-ph/0309028].
- [12] V. Bargmann, *On the Connection between Phase Shifts and Scattering Potential*, Rev. Mod. Phys. **21** (1949) 488.
- [13] K. Hartt, *Pade Phenomenology for NN Scattering: s Wave Singlet Phase Shifts*, Phys. Rev. C **23** (1981) 2399.
- [14] K. Hartt, *Pade phenomenology for two-body bound states*, Phys. Rev. C **26** (1982) 2616.
- [15] V. A. Babenko and N. M. Petrov, *Description of the two-nucleon system on the basis of the Bargmann representation of the S matrix*, Phys. Atom. Nucl. **68** (2005) 219 [nucl-th/0502041].

[16] H. Leeb, S. A. Sofianos, J. M. Sparenberg and D. Baye, *Supersymmetric transformations in coupled channel systems*, Phys. Rev. C **62** (2000) 064003 [nucl-th/0008054].

[17] B. F. Samsonov and F. Stancu, *The Phase shift effective range expansion from supersymmetric quantum mechanics*, Phys. Rev. C **67** (2003) 054005 [nucl-th/0304010].

[18] A. Pupasov, B. Samsonov, J. M. Sparenberg and D. Baye, *Reconstructing the nucleon-nucleon potential by a new coupled-channel inversion method*, Phys. Rev. Lett. **106** (2011) 152301 [arXiv:1101.3691 [nucl-th]].

[19] H. V. von Geramb and H. Kohlhoff, *Nucleon-nucleon potentials from phase shifts inversion*, Lect. Notes Phys. **427** (1994) 285.

[20] H. Kohlhoff and H. V. von Geramb, *Coupled channels Marchenko inversion for nucleon-nucleon potentials*, Lect. Notes Phys. **427** (1994) 314.

[21] J.-M. Sparenberg and D. Baye, *Inverse scattering with singular potentials: A supersymmetric approach*, Phys. Rev. C **55** (1997) 2175.

[22] D. Baye, J. M. Sparenberg, A. M. Pupasov-Maksimov and B. F. Samsonov, *Single- and coupled-channel radial inverse scattering with supersymmetric transformations*, J. Phys. A **47** (2014) 243001 [arXiv:1401.0439 [quant-ph]].

[23] GWDAC (<http://gwdac.phys.gwu.edu/>)

[24] J. J. de Swart, C. P. F. Terheggen and V. G. J. Stoks, *The Low-energy n p scattering parameters and the deuteron*, nucl-th/9509032.

[25] V. A. Babenko and N. M. Petrov, *Determination of the root-mean-square radius of the deuteron from present-day experimental data on neutron-proton scattering*, Phys. Atom. Nucl. **71** (2008) 1730 [Yad. Fiz. **71** (2008) 1761].

[26] M. Garcon and J. W. Van Orden, *The Deuteron: Structure and form-factors*, Adv. Nucl. Phys. **26** (2001) 293 [nucl-th/0102049].

[27] B. F. Samsonov and F. Stancu, *Phase equivalent chains of Darboux transformations in scattering theory*, Phys. Rev. C **66** (2002) 034001, quant-ph/0204112.

[28] I. Gelfand, B. Levitan, *On the determination of a differential equation from its spectral function*, Izvestiya Akad. Nauk SSSR. Ser. Mat. 15, (1951) 309-360. (in Russian)

[29] B. Levitan, *Inverse Sturm-Liouville problems*, VNU Press, Utrecht, 1987.

[30] P. Swan, *Asymptotic phase-shifts and bound states for two-body central interactions*, Nucl. Phys. **46** (1963) 669.

[31] C.-L. Ho, J.-C. Lee and R. Sasaki, *Scattering Amplitudes for Multi-indexed Extensions of Solvable Potentials*, Annals Phys. **343** (2014) 115 [arXiv:1309.5471 [quant-ph]].